ACS APPLIED MATERIALS & INTERFACES

Letter

Cite This: ACS Appl. Mater. Interfaces 2018, 10, 21079−21083

www.acsami.org

Elucidating the Variable-Temperature Mechanical Properties of a Negative Thermal Expansion Metal−Organic Framework

Jurn Heinen,*[,†] Austin D. Ready,[‡] Thomas D. Bennett,[§] David Dubbeldam,[†] Raymond W. Friddle,[‡] and Nicholas C. Burtch*[,‡]

[†]Van't Hoff Institute for Molecular Sciences, University of Amsterdam, Science Park 904, 1098 XH Amsterdam, The Netherlands

[‡]Sandia National Laboratories, 7011 East Avenue, Livermore, California 94551, United States

[§]Department of Materials Science and Metallurgy, University of Cambridge, 27 Charles Babbage Road, Cambridge CB3 0FS, United Kingdom

Supporting Information

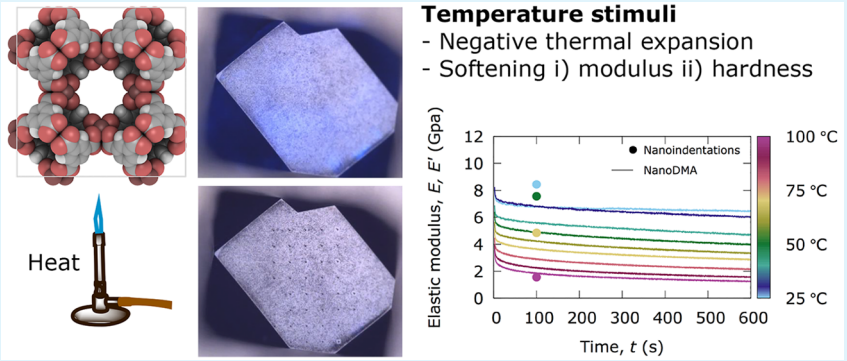

ABSTRACT: We report the first experimental study into the thermomechanical and viscoelastic properties of a metal−organic framework (MOF) material. Nanoindentations show a decrease in the Young's modulus, consistent with classical molecular dynamics simulations, and hardness of HKUST-1 with increasing temperature over the 25−100 °C range. Variable-temperature dynamic mechanical analysis reveals significant creep behavior, with a reduction of 56% and 88% of the hardness over 10 min at 25 and 100 °C, respectively. This result suggests that, despite the increased density that results from increasing temperature in the negative thermal expansion MOF, the thermally induced softening due to vibrational and entropic contributions plays a more dominant role in dictating the material's temperature-dependent mechanical behavior.

KEYWORDS: *dynamic mechanical analysis, nanoindentations, negative thermal expansion, metal−organic frameworks, elasticity, mechanical properties, HKUST-1, molecular dynamics*

Downloaded via UNIV AMSTERDAM on April 17, 2019 at 10:34:32 (UTC).
See https://pubs.acs.org/sharingguidelines for options on how to legitimately share published articles.

Metal−organic frameworks (MOFs) are a fascinating class of nanoporous materials with potential applications ranging from gas storage, separation, and catalysis to sensors and electronic devices.[1,2] A better understanding of their mechanical properties is essential for understanding and optimizing their stability and performance properties in such applications.[3−5] Tensorial analysis of MOF elastic constants using *ab initio* density functional theory (DFT) calculations has shed new light on mechanical properties which may be connected to large-scale flexible modes such as negative thermal expansion (NTE),[6] gate opening,[7] and negative linear compressibility.[8] Experimentally, the bulk moduli and pressure-induced amphorphization behavior can be measured by applying hydrostatic compression in diamond anvil cell experiments.[9] Nanoindentation experiments have been primarily used to measure the Young's modulus and hardness of MOF single crystals and thin films.[3,10−13] The Young's modulus is a measure of a material's reversible response to strain in the Hookean limit, and hardness is related to the irreversible plastic deformation of a material upon strain.[14,15] A recent study by Sun et al. demonstrated that bimodal amplitude modulated−frequency modulated atomic force microscopy can be used to measure the Young's moduli of microcrystalline MOF nanoparticles.[16] Zeng and Tan showed that the use of high unloading strain rates using atomic force microscopy (AFM) nanoindentations can yield accurate Young's moduli for micron-sized crystals as well.[17]

Most nanoindentation studies rely on the Oliver−Pharr analysis of the load−displacement curves by assuming that the deformation is within the Hookean limit of the material.[18] These experiments neglect the time-dependent deformation of the material, known as creep. From an application's perspective, it is important that creep effects due to viscoelasticity as well as

Received: April 24, 2018
Accepted: June 6, 2018
Published: June 6, 2018

© 2018 American Chemical Society

DOI: 10.1021/acsami.8b06604
ACS Appl. Mater. Interfaces 2018, 10, 21079−21083

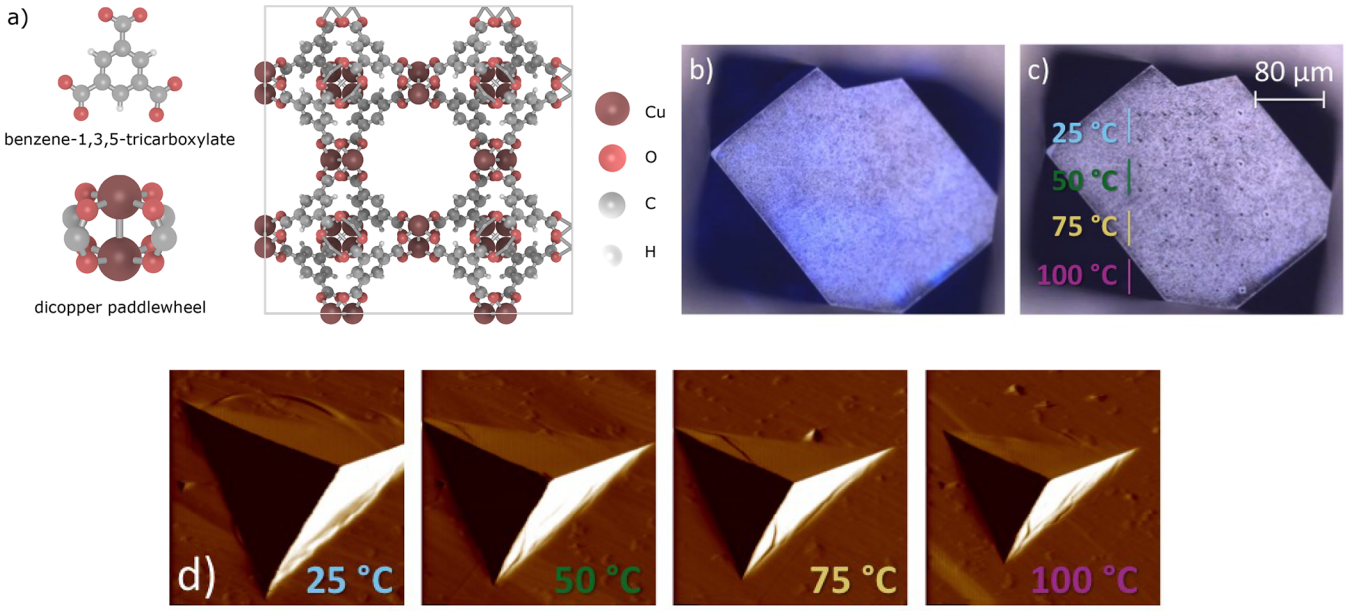

Figure 1. (a) Building units of HKUST-1 and ball-and-stick model of the unit cell along the ⟨100⟩ direction. Optical images of a (b) preactivated and (c) *in situ* activated HKUST-1 crystal facet with residual indents. (d) AFM images of representative residual indents (scan size: 10 × 10 μm).

temperature effects be better understood. To our knowledge, the thermomechanical properties of MOFs have only been studied computationally. For example, classical and *ab initio* simulations on IRMOF-1 showed a decrease in the elastic constants with increasing temperature.[19−21] This behavior was also reported for other materials that exhibit negative thermal expansion (NTE), such as ZrW_2O_8.[22,23] This observation is consistent with the understanding that materials tend to become more elastic and exhibit a reduction in their elastic constants with increasing temperature.[24−27]

Here, we study the viscoelastic and thermomechanical properties of the NTE MOF HKUST-1[28] using variable-temperature dynamic mechanical analysis (DMA)[29] and nanoindentations combined with differential scanning calorimetry−thermogravimetric analysis and classical molecular dynamics simulations. HKUST-1 consists of dicopper paddlewheels interconnected by BTC (BTC = benzene-1,3,5-tricarboxylate) linkers, as shown in Figure 1a, and has a linear coefficient of thermal expansion $\alpha_l \approx -4.5 \times 10^{-6}$ K^{-1}.[30,31] HKUST-1 is a prototypical structure that has also been studied for its utility in humidity sensing devices, including in microcantilever sensors where the material's Young's modulus has a direct bearing on the sensor's sensitivity.[32] Further, the hardness can be related to the scratch resistance of a material, which has important implications for determining suitable handling and processing conditions for its use in electronic devices.[33] In this work, we considered temperatures up to 100 °C because of the reported irreversible changes to HKUST-1 lattice parameters above ∼127 °C.[30] Qualitative agreement between the variable-temperature behavior of the elastic moduli from the experimental nanoindentation and DMA experiments is obtained and is also supported by complementary classical molecular dynamics simulations.

Single crystals of HKUST-1 were synthesized solvothermally according to literature procedures.[34] X-ray diffraction patterns (Figure S1) and N_2 adsorption isotherms (Figure S2) were recorded to characterize the HKUST-1 crystals. All mechanical properties were measured using a Hysitron TI 950 nanoindentor (load-controlled) utilizing a xSol 600 temperature control stage with a diamond Berkovich tip. Single crystals were glued on glass slides, and the crystals were activated *in situ* under nitrogen flow at 100 °C for 1 h, using a ramp rate of 10 °C/min from room temperature, until the blue to purple color change indicative of solvent removal was observed (Figures 1b and 1c).[35,36] Combined differential scanning calorimetry−thermogravimetric analysis showed no thermal transition over the 25−100 °C temperature range (Figures S3 and S4). Figure S6 shows additional time-dependent optical images obtained during activation. The Young's modulus E and hardness H values were obtained from repeated measurements of load−displacement curves, following the Oliver−Pharr method.[18] DMA measurements were performed under a nitrogen flow by measuring the storage modulus E' and hardness values with a constant load of P = 3000 μN, an amplitude of 50 μN, and a frequency of 220 Hz. The available surface area on an individual crystal's facet required that measurements with each of the different techniques be performed on different single crystals, in order to minimize effects due to adjacent residual indents. Variable-temperature measurements that were reported for a given technique, however, were all performed on the same crystal facet. Classical molecular dynamics simulations were performed using the RASPA-2.0 code to obtain finite-temperature elastic constants.[37]

To convert the indentation modulus to the Young's modulus, the Poisson's ratio proposed by Bundschuh et al. of ν = 0.433 was used.[11] Under this assumption, our indentation modulus of 7.88 ± 1.15 GPa at room temperature produces a Young's modulus of E = 6.45 ± 0.94 GPa (averaged over indents from 4000 to 8000 μN). This value is lower than those obtained for HKUST-1 thin films (Bundschuh et al.:[11] 9.3 GPa) and monoliths (Tian et al.:[38] 9.3 ± 0.3 GPa). The choice of the Poisson's ratio of the sample can significantly influence the Young's modulus for MOF materials, however.[39] For example, a value of ν = 0.02 gives E = 7.09 ± 0.85 GPa, which is in reasonable agreement with the theoretical value of E = 8.1 GPa.[6]

DOI: 10.1021/acsami.8b06604
ACS Appl. Mater. Interfaces 2018, 10, 21079−21083

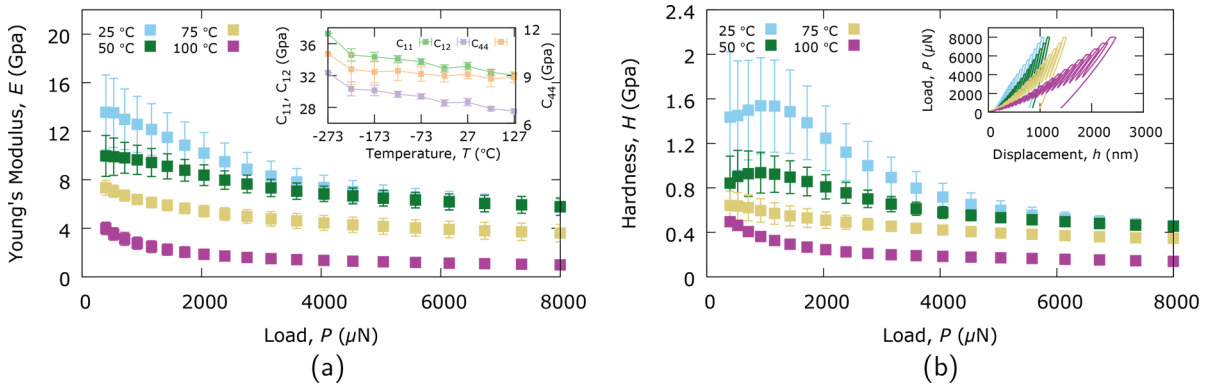

Figure 2. (a) Young's modulus as a function of load at various temperatures. Inset: variable-temperature elastic constants obtained from classical molecular dynamics simulations. Lines are guidance to the eye. (b) Hardness as a function of load at various temperatures. Inset: representative load−displacement curves for each temperature. Error bars of nanoindentations are standard deviations of ten indents for each temperature on the same crystal facet.

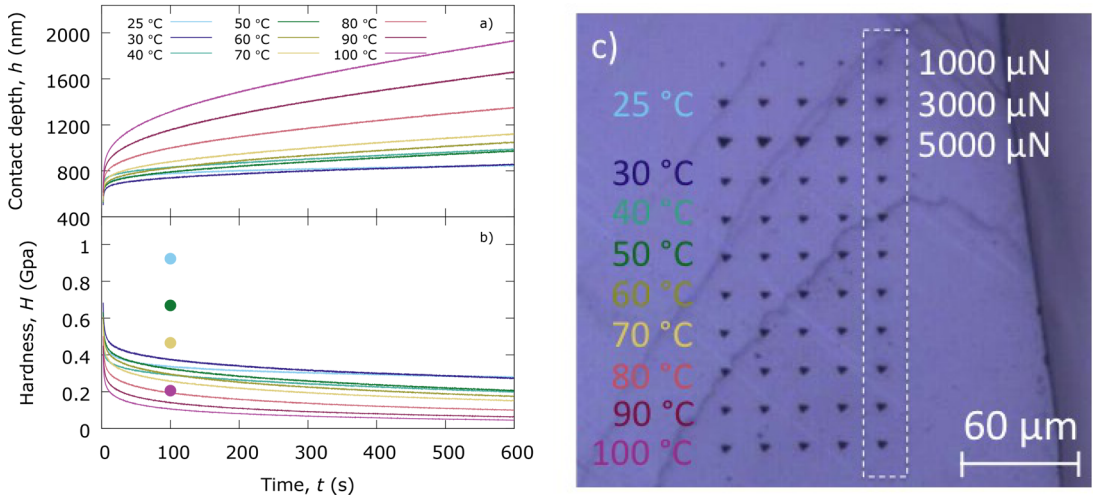

Figure 3. Time evolution from 25 to 100 °C of the (a) contact depth and (b) hardness. Each temperature corresponds to a different position on the crystal facet. Circles are hardness values from previous nanoindentation experiments at P = 3000 μN. (c) Optical image of crystal facets subjected to creep analysis tests. Creep results are from indents in dashed rectangle at P = 3000 μN.

After *in situ* activation, the material becomes harder and less elastic, as can been seen from Figure S7. It is known that upon solvent evacuation the HKUST-1 unit cell shrinks, and the framework thus becomes more dense.[36] A more dense material would be consistent with an increased degree of resistance from the framework surface toward deformation by the indenter tip. Upon increasing temperature an NTE material undergoes a contraction, and representative AFM images show smaller residual indents at higher temperatures (Figure 1d) suggesting that the material becomes harder. However, variable-temperature Young's modulus and hardness as a function of applied load, shown in Figure 2, obtained from nanoindentations show the opposite behavior. We find that the Young's modulus decreases to 6.28 ± 0.72, 3.99 ± 0.70, and 1.16 ± 0.34 at T = 50, 75, and 100 °C, respectively. Variable-temperature elastic constants from classical molecular dynamics simulations (inset of Figure 2a) confirm softening of the material with increasing temperature. From recent *ab inito* molecular dynamics simulations, softening of the elastic constants upon temperature stimuli was also observed for IRMOF-1 and UiO-66.[21] While the effects of temperature on the simulated and experimental moduli values are qualitatively consistent, the quantitative differences between these results can be explained by the employed force field not being parametrized on the material's mechanical properties and that the simulated (bulk) values are calculated in the limit of zero strain, whereas moduli obtained from indentation experiments are at finite strains. Most solids exhibit a zero slope in their elastic properties at cryogenic temperatures, such as MgO[40] and copper.[27] However, interestingly, HKUST-1 exhibits a decay of its calculated isothermal elastic constants at these temperatures.

A similar correlation is also observed for the hardness (Figure 2b), where we find the maximum displacement at constant load increases with increasing temperature, as can be seen from representative load−displacement curves at the inset of Figure 2b (also see Figure S8). Similarly, a 34−46% reduction of the hardness over a 10−70 °C temperature interval has been reported for several molecular crystals[41] as well as a 60% hardness reduction of Au thin films over a temperature range of 20−130 °C.[42] We find that the residual indents, however, as observed from the AFM images, become smaller at higher temperatures. This seemingly contradicts the decrease in hardness that we observe but can be better understood through the Young's modulus and viscoelastic analysis that is investigated through the DMA experiments in the following section.

DOI: 10.1021/acsami.8b06604
ACS Appl. Mater. Interfaces 2018, 10, 21079−21083

Variable-temperature creep tests using DMA experiments were performed on a separate single crystal. Figure 3a and 3b show the time evolution of the contact depth and hardness, respectively, for nine creep measurements, with each measurement representing a different temperature in the interval of 25−100 °C. The residual indents from these measurements are shown in Figure 3c. We find that the amount of creep, captured by the increase in contact depth over time, becomes increasingly larger at higher temperatures. This time-dependent creep has a considerable impact on the mechanical properties, with the hardness (Figure 3b) decaying from ∼0.64 to 0.28 GPa and from ∼0.40 to 0.05 GPa after only 10 min at 25 and 100 °C, respectively, as the contact depth increases over time. This is consistent with the quasistatic nanoindentation results, where at higher loads the indent displacement becomes larger and the hardness decreases (see Figure 2b). The relative change of the hardness over time increases with increasing temperature. The storage modulus E', related to the energy stored in the material, follows a similar trend as the hardness and Young's modulus from nanoindentations (Figure S10a). The $\tan(\delta)$-value, which is a measurement of the viscoelasticity of a material, does not change appreciably over time. At room temperature, $\tan(\delta) = 0.032 \pm 0.004$, and this increases at T = 100 °C to 0.096 ± 0.002, indicating that the viscous contributions increase relative to the elastic contributions in the material with increasing temperatures (Figure S10b).

To conclude, quasistatic nanoindentations, DMA experiments, and classical molecular simulations show softening of HKUST-1 at increasing temperature, despite the material exhibiting NTE. The creep behavior we observe is substantial, with a reduction of 56% and 88% in the hardness after 10 min at 25 and 100 °C, respectively. This first experimental study into the temperature dependency of MOF elasticity and hardness properties provides important insight into the expected stability and performance characteristics of a negative thermal expansion MOF for a number of applications where a comprehensive mechanical property understanding is critical.

■ ASSOCIATED CONTENT

Supporting Information

The Supporting Information is available free of charge on the ACS Publications website at DOI: 10.1021/acsami.8b06604.

Synthesis procedure, powder X-ray diffraction patterns, N_2 adsorption isotherm at 77 K, DSC-TGA results, optical images illustrating color changes during activation, load−displacement curves of nanoindentation measurements, storage modulus, and $\tan(\delta)$ values from dynamic mechanical analysis and simulation details (PDF)

■ AUTHOR INFORMATION

Corresponding Authors

*E-mail: j.heinen@uva.nl.
*E-mail: nburtch@sandia.gov.

ORCID

Jurn Heinen: 0000-0001-8838-5213
Thomas D. Bennett: 0000-0003-3717-3119
David Dubbeldam: 0000-0002-4382-1509
Nicholas C. Burtch: 0000-0003-0052-7307

Notes

The authors declare no competing financial interest.

■ ACKNOWLEDGMENTS

N.C.B. acknowledges the support of the Sandia National Laboratories Truman Fellowship Program, and N.C.B. and R.W.F. acknowledge support by the Sandia National Laboratories Laboratory Directed Research and Development (LDRD) Program. Sandia National Laboratories is a multimission laboratory managed and operated by National Technology and Engineering Solutions of Sandia, LLC, a wholly owned subsidiary of Honeywell International, Inc., for the U.S. Department of Energy's National Nuclear Security Administration under contract DE-NA0003525. T.D.B. acknowledges the support of the Royal Society for a University Research Fellowship. J.H. acknowledges the support of the University of Amsterdam for an UvA385 grant. We acknowledge Jonathan Zimmerman for fruitful discussions. This paper describes objective technical results and analysis. Any subjective views or opinions that might be expressed in the paper do not necessarily represent the views of the U.S. Department of Energy or the United States Government.

■ REFERENCES

(1) Kitagawa, S.; Kitaura, R.; Noro, S.-i. Functional Porous Coordination Polymers. *Angew. Chem., Int. Ed.* **2004**, *43*, 2334−2375.
(2) Zhou, H.-C.; Long, J. R.; Yaghi, O. M. Introduction to Metal-Organic Frameworks. *Chem. Rev.* **2012**, *112*, 673−674.
(3) Tan, J. C.; Cheetham, A. K. Mechanical Properties of Hybrid Inorganic-Organic Framework Materials: Establishing Fundamental Structure-Property Relationships. *Chem. Soc. Rev.* **2011**, *40*, 1059−1080.
(4) Burtch, N. C.; Heinen, J.; Bennett, T. D.; Dubbeldam, D.; Allendorf, M. D. Mechanical Properties in Metal-Organic Frameworks: Emerging Opportunities and Challenges for Device Functionality and Technological Applications. *Adv. Mater.* **2017**, *0*, 1704124.
(5) Rogge, S. M. J.; Waroquier, M.; Van Speybroeck, V. Reliably Modeling the Mechanical Stability of Rigid and Flexible Metal-Organic Frameworks. *Acc. Chem. Res.* **2018**, *51*, 138−148.
(6) Ryder, M. R.; Civalleri, B.; Cinque, G.; Tan, J.-C. Discovering Connections between Terahertz Vibrations and Elasticity Underpinning the Collective Dynamics of the HKUST-1 Metal-Organic Framework. *CrystEngComm* **2016**, *18*, 4303−4312.
(7) Ryder, M. R.; Civalleri, B.; Bennett, T. D.; Henke, S.; Rudić, S.; Cinque, G.; Fernandez-Alonso, F.; Tan, J.-C. Identifying the Role of Terahertz Vibrations in Metal-Organic Frameworks: From Gate-Opening Phenomenon to Shear-Driven Structural Destabilization. *Phys. Rev. Lett.* **2014**, *113*, 215502.
(8) Ortiz, A. U.; Boutin, A.; Fuchs, A. H.; Coudert, F.-X. Anisotropic Elastic Properties of Flexible Metal-Organic Frameworks: How Soft are Soft Porous Crystals? *Phys. Rev. Lett.* **2012**, *109*, 195502.
(9) Gándara, F.; Bennett, T. D. Crystallography of Metal-Organic Frameworks. *IUCrJ* **2014**, *1*, 563−570.
(10) Bahr, D. F.; Reid, J. A.; Mook, W. M.; Bauer, C. A.; Stumpf, R.; Skulan, A. J.; Moody, N. R.; Simmons, B. A.; Shindel, M. M.; Allendorf, M. D. Mechanical Properties of Cubic Zinc Carboxylate IRMOF-1 Metal-Organic Framework Crystals. *Phys. Rev. B: Condens. Matter Mater. Phys.* **2007**, *76*, 184106.
(11) Bundschuh, S.; Kraft, O.; Arslan, H. K.; Gliemann, H.; Weidler, P. G.; Wöll, C. Mechanical Properties of Metal-Organic Frameworks: An Indentation Study on Epitaxial Thin Films. *Appl. Phys. Lett.* **2012**, *101*, 101910.
(12) Henke, S.; Li, W.; Cheetham, A. K. Guest-Dependent Mechanical Anisotropy in Pillared-Layered Soft Porous Crystals - A Nanoindentation Study. *Chem. Sci.* **2014**, *5*, 2392−2397.
(13) Li, W.; Henke, S.; Cheetham, A. K. Research Update: Mechanical Properties of Metal-Organic Frameworks - Influence of Structure and Chemical Bonding. *APL Mater.* **2014**, *2*, 123902.

DOI: 10.1021/acsami.8b06604
ACS Appl. Mater. Interfaces 2018, 10, 21079−21083

(14) Varughese, S.; Kiran, M. S. R. N.; Ramamurty, U.; Desiraju, G. R. Nanoindentation in Crystal Engineering: Quantifying Mechanical Properties of Molecular Crystals. *Angew. Chem., Int. Ed.* **2013**, *52*, 2701−2712.
(15) Ramamurty, U.; Jang, J.-i. Nanoindentation for probing the mechanical behavior of molecular crystals-a review of the technique and how to use it. *CrystEngComm* **2014**, *16*, 12−23.
(16) Sun, Y.; Hu, Z.; Zhao, D.; Zeng, K. Mechanical Properties of Microcrystalline Metal-Organic Frameworks (MOFs) Measured by Bimodal Amplitude Modulated-Frequency Modulated Atomic Force Microscopy. *ACS Appl. Mater. Interfaces* **2017**, *9*, 32202−32210.
(17) Zeng, Z.; Tan, J.-C. AFM Nanoindentation To Quantify Mechanical Properties of Nano- and Micron-Sized Crystals of a Metal-Organic Framework Material. *ACS Appl. Mater. Interfaces* **2017**, *9*, 39839−39854.
(18) Oliver, W.; Pharr, G. An Improved Technique for Determining Hardness and Elastic Modulus using Load and Displacement Sensing Indentation Experiments. *J. Mater. Res.* **1992**, *7*, 1564−1583.
(19) Han, S. S.; Goddard, W. A. Metal-Organic Frameworks Provide Large Negative Thermal Expansion Behavior. *J. Phys. Chem. C* **2007**, *111*, 15185−15191.
(20) Greathouse, J. A.; Allendorf, M. D. Force Field Validation for Molecular Dynamics Simulations of IRMOF-1 and Other Isoreticular Zinc Carboxylate Coordination Polymers. *J. Phys. Chem. C* **2008**, *112*, 5795−5802.
(21) Banlusan, K.; Strachan, A. First-Principles Study of Elastic Mechanical Eesponses to Applied Deformation of Metal-Organic Frameworks. *J. Chem. Phys.* **2017**, *146*, 184705.
(22) Evans, J. S. O.; David, W. I. F.; Sleight, A. W. Structural Investigation of the Negative-Thermal-Expansion Material ZrW_2O_8. *Acta Crystallogr., Sect. B: Struct. Sci.* **1999**, *55*, 333−340.
(23) Drymiotis, F. R.; Ledbetter, H.; Betts, J. B.; Kimura, T.; Lashley, J. C.; Migliori, A.; Ramirez, A. P.; Kowach, G. R.; Van Duijn, J. Monocrystal Elastic Constants of the Negative-Thermal-Expansion Compound Zirconium Tungstate (ZrW_2O_8). *Phys. Rev. Lett.* **2004**, *93*, 025502.
(24) Andrews, J. P. The Variation of Young's Modulus at High Temperatures. *Proc. Phys. Soc. London* **1924**, *37*, 169.
(25) Kimball, A. L.; Lovell, D. E. Variation of Young's Modulus with Temperature From Vibration Measurements. *Phys. Rev.* **1925**, *26*, 121−124.
(26) Wachtman, J. B.; Tefft, W. E.; Lam, D. G.; Apstein, C. S. Exponential Temperature Dependence of Young's Modulus for Several Oxides. *Phys. Rev.* **1961**, *122*, 1754−1759.
(27) Ledbetter, H. Sound Velocities, Elastic Constants: Temperature Dependence. *Mater. Sci. Eng., A* **2006**, *442*, 31−34.
(28) Chui, S.; Lo, S.; Charmant, J.; Orpen, A.; Williams, I. A Chemically Functionalizable Nanoporous Material [Cu-3(TMA)(2)(H2O)(3)](n). *Science* **1999**, *283*, 1148−1150.
(29) Menard, K. P. *Dynamic Mechanical Analysis: A Practical Introduction*; CRC Press, 1999.
(30) Wu, Y.; Kobayashi, A.; Halder, G.; Peterson, V.; Chapman, K.; Lock, N.; Southon, P.; Kepert, C. Negative Thermal Expansion in the Metal-Organic Framework Material Cu3(1,3,5-benzenetricarboxylate)-2. *Angew. Chem., Int. Ed.* **2008**, *47*, 8929−8932.
(31) Peterson, V.; Kearley, G.; Wu, Y.; Ramirez-Cuesta, A.; Kemner, E.; Kepert, C. Local Vibrational Mechanism for Negative Thermal Expansion: A Combined Neutron Scattering and First-Principles Study. *Angew. Chem., Int. Ed.* **2010**, *49*, 585−588.
(32) Venkatasubramanian, A.; Lee, J.-H.; Stavila, V.; Robinson, A.; Allendorf, M. D.; Hesketh, P. J. MOF @ MEMS: Design Optimization for High Sensitivity Chemical Detection. *Sens. Actuators, B* **2012**, *168*, 256−262.
(33) Stassen, I.; Burtch, N.; Talin, A.; Falcaro, P.; Allendorf, M.; Ameloot, R. An Updated Roadmap for the Integration of Metal-Organic Frameworks with Electronic Devices and Chemical Sensors. *Chem. Soc. Rev.* **2017**, *46*, 3185−3241.
(34) Tovar, T. M.; Zhao, J.; Nunn, W. T.; Barton, H. F.; Peterson, G. W.; Parsons, G. N.; LeVan, M. D. Diffusion of CO2 in Large Crystals of Cu-BTC MOF. *J. Am. Chem. Soc.* **2016**, *138*, 11449−11452.
(35) Schlichte, K.; Kratzke, T.; Kaskel, S. Improved Synthesis, Thermal Stability and Catalytic Properties of the Metal-Organic Framework Compound Cu3(BTC)2. *Microporous Mesoporous Mater.* **2004**, *73*, 81−88.
(36) Prestipino, C.; Regli, L.; Vitillo, J. G.; Bonino, F.; Damin, A.; Lamberti, C.; Zecchina, A.; Solari, P. L.; Kongshaug, K. O.; Bordiga, S. Local Structure of Framework Cu(II) in HKUST-1 Metallorganic Framework: Spectroscopic Characterization upon Activation and Interaction with Adsorbates. *Chem. Mater.* **2006**, *18*, 1337−1346.
(37) Dubbeldam, D.; Calero, S.; Ellis, D. E.; Snurr, R. Q. RASPA: Molecular Simulation Software for Adsorption and Diffusion in Flexible Nanoporous Materials. *Mol. Simul.* **2016**, *42*, 81−101.
(38) Tian, T.; Zeng, Z.; Vulpe, D.; Casco, M. E.; Divitini, G.; Midgley, P. A.; Silvestre-Albero, J.; Tan, J.-C.; Moghadam, P. Z.; Fairen-Jimenez, D. A Sol-Gel Monolithic Metal-Organic Framework with Enhanced Methane Uptake. *Nat. Mater.* **2017**, *17*, 174−179.
(39) Tan, J.-C.; Civalleri, B.; Lin, C.-C.; Valenzano, L.; Galvelis, R.; Chen, P.-F.; Bennett, T. D.; Mellot-Draznieks, C.; Zicovich-Wilson, C. M.; Cheetham, A. K. Exceptionally Low Shear Modulus in a Prototypical Imidazole-Based Metal-Organic Framework. *Phys. Rev. Lett.* **2012**, *108*, 095502.
(40) Anderson, O. L. Derivation of Wachtman's Equation for the Temperature Dependence of Elastic Moduli of Oxide Compounds. *Phys. Rev.* **1966**, *144*, 553−557.
(41) Mohamed, R. M.; Mishra, M. K.; AL-Harbi, L. M.; Al-Ghamdi, M. S.; Asiri, A. M.; Reddy, C. M.; Ramamurty, U. Temperature Dependence of Mechanical Properties in Molecular Crystals. *Cryst. Growth Des.* **2015**, *15*, 2474−2479.
(42) Volinsky, A. A.; Moody, N. R.; Gerberich, W. W. Nanoindentation of Au and Pt/Cu thin films at elevated temperatures. *J. Mater. Res.* **2004**, *19*, 2650−2657.

DOI: 10.1021/acsami.8b06604
ACS Appl. Mater. Interfaces 2018, 10, 21079−21083